Development and Analysis of a Pole-Changing Winding Configuration for Energy-Efficient Multi-Speed Ventilation Motor Drives

Dauletbek Rismukhamedov[1], Khusniddin Shamsutdinov[2], Khayotullo Magdiev[3], Sarvar Ganiev[1] and Shakhobiddin Khusanov[1]

[1]*Department Department of Electrical Engineering and Electrical Mechanics, Almalyk State Technical Institute, Mirzo Ulugbek Str. 45, 110100 Almalyk, Uzbekistan*

[2]*Department of Power Plants, Networks and Systems, Tashkent State Technical University named after Islam Karimov, Universitet Str. 2, 100095 Tashkent, Uzbekistan*

[3]*Department of Natural Sciences, Shakhrisabz State Pedagogical Institute, Shakhrisabz Str. 10, 180600 Shakhrisabz, Uzbekistan*

rdaman@mail.ru, shamsutdinovh83@gmail.com, zhmagdiyev@gmail.com, shahobiddinhusanov9@gmail.com, ganiyev_st@mail.ru

Keywords: Electric Drive, Slots, Stator, Pole, Winding, Pole-Changing Winding, Single-Speed, Winding Scheme, Differential Leakage Factor.

Abstract: Worldwide research is increasingly focused on the development of adjustable electric drives for ventilation systems that ensure stable and controllable microclimate parameters while reducing energy and resource consumption. Ventilation systems are among the most energy-intensive components of industrial and agricultural facilities, particularly in poultry farming, where continuous air exchange is required to maintain optimal environmental conditions. In this context, one of the priority scientific and engineering tasks is the design of automatically controlled multi-speed electric drives based on motors with improved energy performance that fully meet the operational requirements of fan-type electric drives. This paper presents the development and analysis of a new pole-changing winding configuration for multi-speed asynchronous motors intended for ventilation systems. An enhanced Y/YY winding scheme with additional branches is proposed, enabling more efficient utilization of the motor's active part and a reduction in copper and insulation material consumption. Furthermore, a novel 8/4 pole-changing winding based on the method of discretely defined spatial functions is developed. The proposed approach allows the synthesis of winding schemes with electromagnetic characteristics close to those of conventional windings while providing improved flexibility in speed control. The harmonic composition of the magnetomotive force, winding factors, and differential leakage coefficients are analyzed, confirming the high electromagnetic symmetry and energy efficiency of the proposed solution. The obtained results demonstrate that the developed winding scheme significantly improves the performance and energy efficiency of fan-type electric drives and can be effectively applied in energy-saving ventilation systems.

1 INTRODUCTION

Worldwide, poultry meat production accounts for 29.3% of the total meat output. In poultry meat production, electricity costs account for approximately 12-14% of total expenses. Due to the high energy consumption in the poultry sector, special attention is given to energy-saving issues. At present, developed countries are conducting scientific research on improving production efficiency and automating technological processes, as well as on the introduction of new technologies into production [1]. In this regard, taking into account the specific features of technological processes in poultry houses, special importance is attached to enhancing the energy efficiency of the microclimate system through the improvement of ventilation devices with the application of automatic control.

In this direction, one of the priority tasks is the development of automatically controlled electric drives based on multi-speed motors with improved energy performance that meet the requirements for fan drives. At the same time, one of the pressing tasks is the development of new pole-changing winding schemes with high electromagnetic properties and simple manufacturing technology for use in multi-speed motors [2], [3].

Based on the analysis of energy consumption of the microclimate system in the broiler shop of LLC "VARGANZA PARRANDASI", it was found that the total annual electricity consumption amounts to 297.084 kWh, including 160.284 kWh by the ventilation system, 17.280 kWh by the electric lighting system, 72.000 kWh by the electric heating system, and 47.520 kWh by the cooling system. Figure 1 shows the annual electricity consumption distribution of the microclimate system in the broiler shop of LLC "VARGANZA PARRANDASI", where the ventilation system accounts for the largest share. Improving its efficiency, namely addressing energy-saving tasks, has been defined as the primary goal of the scientific research.

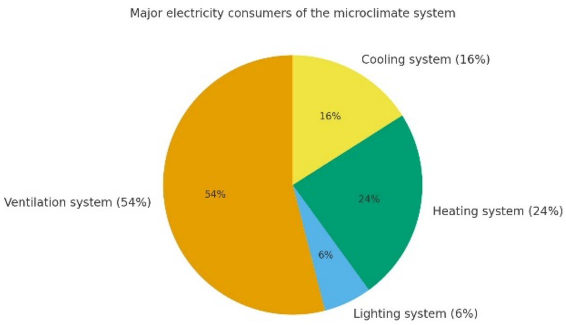

Figure 1: Annual electricity consumption of the microclimate system in the broiler shop of LLC "VARGANZA PARRANDASI".

It is known that a ventilation system with single-speed fans operating at a speed of 1500 rpm provides the required air flow velocity at the expense of high electricity consumption [4], [5]. As can be seen from Figure 2, the use of multi-speed fans at different speeds makes it possible to provide the required air flow velocity with significantly lower electricity consumption.

As a result of studying the existing ventilation system at LLC "VARGANZA PARRANDASI", it was found that the introduction of fan units equipped with pole-changing three-speed motors with an automatic control system, which have lower operating costs and high efficiency, is considered appropriate.

Most multi-speed asynchronous motors used in fans have two or more windings on their stators, which reduces their weight, size, and energy efficiency [4], [6].

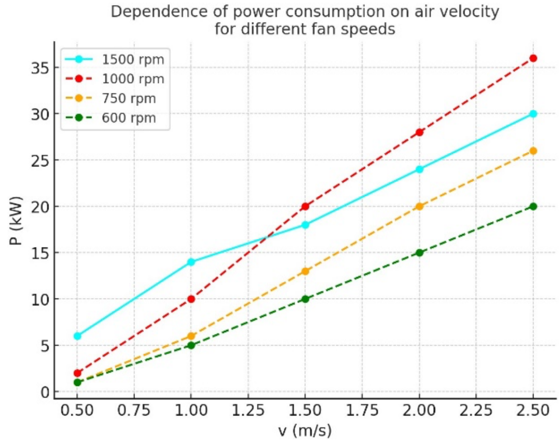

Figure 2: Graph of the dependence of the power consumption of ventilation equipment on the required air flow velocity in the poultry house.

The use of a single pole-changing winding (PCW) with two output groups per pole in multi-speed motors makes it possible to utilize the active part of the machine more efficiently, save winding copper and insulation materials, and increase energy efficiency. This also brings the weight and dimensions of a multi-speed motor closer to those of a simple single-speed asynchronous motor [7], [8].

2 METHODS

Pole-changing winding schemes, which are close in electromagnetic and technological properties to conventional schemes, can be obtained using the method of Discrete Specified Spatial Functions (DSSF). This method was developed by Professor Kh.G. Karimov and was initially applied to the construction of matching coils of contactless asynchronous machines. Later, it was widely used for the development of pole-changing windings [2], [9].

The method is based on a new principle: two simple double-layer lap windings are taken, with the number of pole pairs equal to p_1 and p_2, and the number of phases equal to m_1 and m_2.

These windings are simultaneously applied in the process of designing a two-speed winding. In this case, the scheme for connecting and disconnecting the winding is not adopted in a ready-made form but is generated directly during its construction, or it is selected from a set of previously known basic schemes, taking into account the distribution of phase currents along the motor slots for each pole and the combination of matching winding phases [9].

For the development of a pole-changing winding for the motors of electric drives in ventilation systems of poultry farms, axial fans of the VO-06-300 type are selected, with the number of stator slots equal to 36, and with the pole ratio $2p_1/2p_2$=8/4, producing two speeds, and $2p_3$=6, producing a third speed. In this case, for the formation of two speeds, the current distribution of double-layer stator lap windings is used, while for the formation of the third speed, single-layer stator lap windings of the standard design are applied [10], [11]. On the side of p_1=4 pole pairs, a DSSF 2m-zone winding with the number of stator slots per pole and phase q_1=2 is taken; on the side of p_2=2, an m-zone winding with q_2=3; and on the side of p_3=3, a 2m-zone winding with q_3=2. Tables 1-3 present the DSSF of the lower layer for each pair of poles of the 4/3/2 winding, with a spatial shift between adjacent slots and phases [11]-[13].

As can be seen from the DSSF, the shift angles of these windings do not differ from those of the conventional 2m-zone and m-zone windings, i.e., in all slots the following equality holds: $|\Delta\varphi|=|\varphi_{normal}-\varphi_{PCHW}|=0$.

Based on the DSSF of the lower layer of the windings presented in Tables 1 and 3, the synthesis of the DSSF for the p_1=4 pole winding is carried out in accordance with the newly developed basic "Y/YY with additional branches" scheme, in comparison with the p_2=2 pole winding [14].

Figure 3 shows the distribution of coils among the branches of the basic pole-changing winding (PCW) scheme "Y/YY with additional branches".

The synthesis process is based on the principle of approximating the current distribution and the MMF pattern of the synthesized winding to the current distribution and MMF pattern of a typical winding [14]-[16].

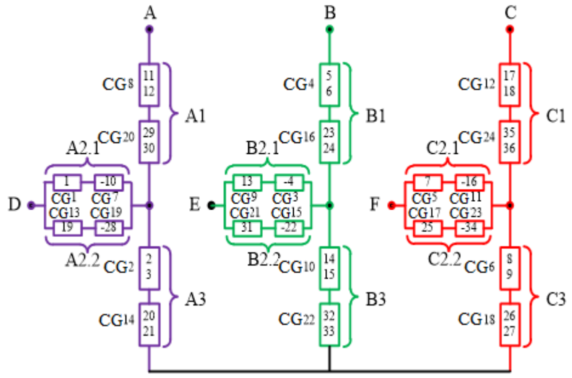

Figure 3: Electrical connection diagram of a pole-changing stator winding with an 8/4 pole ratio.

Table 1: Lower layer of the DSSF winding for p = 4.

1	2	3	4	5	6	7	8	9	10	11	12	13	14	15	16	17	18	19	20	21	22	23	24		36	slots
a	a	a	b	b	b	c	c	c	a	a	a	b	b	b	c	c	c	a	a	a	b	b	b	…	c	p_1=4
0º	0º	0º	0º	60º	60º	60º	60º	120º	120º	120º	120º	180º	180º	180º	180º	240º	240º	240º	240º	300º	300º	300º	300º	…	300º	shift angle
0	0	0	0	0	0	0	0	0	0	0	0	0	0	0	0	0	0	0	0	0	0	0	0	…	0	|Δφ|

Table 2: Lower layer of the DSSF winding for p = 3.

1	2	3	4	5	6	7	8	9	10	11	12	13	14	15	16	17	18	19	20	21	22	23	24		36	slots
d	d	e	e	f	f	d	d	e	e	f	f	d	d	e	e	f	f	d	d	e	e	f	f	…	f	p3=3
0º	0º	0º	0º	240º	240º	240º	240º	120º	120º	120º	120º	0º	0º	0º	0º	240º	240º	240º	240º	120º	120º	120º	120º	…	120º	shift angle
0	0	0	0	0	0	0	0	0	0	0	0	0	0	0	0	0	0	0	0	0	0	0	0	…	0	|Δφ|

Table 3: Lower layer of the DSSF winding for p = 2.

1	2	3	4	5	6	7	8	9	10	11	12	13	14	15	16	17	18	19	20	21	22	23	24		36	slots
d	d	d	e	e	e	f	f	f	d	d	d	e	e	e	f	f	f	d	d	d	e	e	e	…	f	p2=2
0º	0º	0º	0º	240º	240º	240º	240º	120º	120º	120º	120º	0º	0º	0º	0º	240º	240º	240º	240º	120º	120º	120º	120º	…	120º	shift angle
0	0	0	0	0	0	0	0	0	0	0	0	0	0	0	0	0	0	0	0	0	0	0	0	…	0	|Δφ|

Table 4: DSSF of the lower layers with consideration of coil outputs into additional branches.

1	2	3	4	5	6	7	8	9	10	11	12	13	14	15	16	17	18	19	20	21	22	23	24		36	slots
x	a	a	x	b	b	x	c	c	x	a	a	x	b	b	x	c	c	x	a	a	x	b	b	…	c	p_1=4
d	d	d	e	e	e	f	f	f	d	d	d	e	e	e	f	f	f	d	d	d	e	e	e	…	f	p_2=2

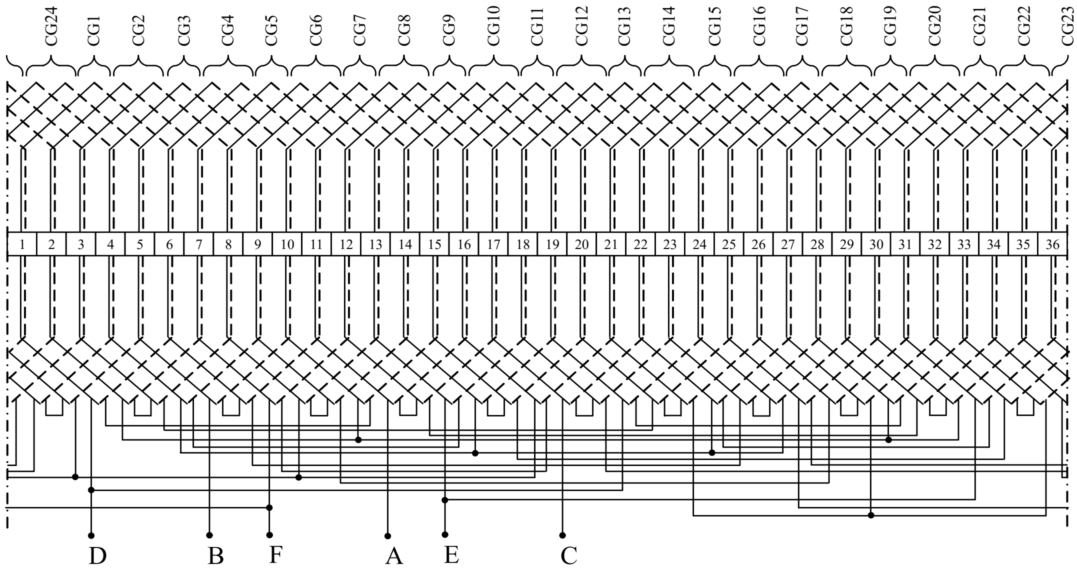

Figure 4: A detailed schematic diagram of a pole-changing winding with an 8/4 pole ratio.

Figure 4 illustrates the detailed schematic of the pole-changing winding with an 8/4 pole ratio.

The winding obtained as a result of the synthesis is brought to the basic scheme “YY/Y with additional branches”, and the cells with coils connected to the additional branches are marked with the symbol (x) (Table 4)

According to the obtained DSSF, the coils are distributed across the branches and a connection scheme of the PCW is constructed, where branches A1, A2, A3 correspond to the first phase, branches B1, B2, B3 to the second phase, and branches C1, C2, C3 to the third phase [11].

In section A1, the coils numbered 11, 12, 29, and 30 are connected in series.

Section A2 is divided into two parts: A2.1, which includes coils 1 and 10, and A2.2, which includes coils 19 and 28. The coils in each subgroup are connected in parallel.

In section A3, the coils numbered 2, 3, 20, and 21 are connected in series.

In section B1, the coils numbered 5, 6, 23, and 24 are connected in series.

Section B2 is divided into two parts: B2.1, which includes coils 13 and 4, and B2.2, which includes coils 31 and 22. The coils in each subgroup are connected in parallel.

In section B3, the coils numbered 14, 15, 32, and 33 are connected in series.

In section C1, the coils numbered 17, 18, 35, and 36 are connected in series.

Section C2 is divided into two parts: C2.1, which includes coils 7 and 16, and C2.2, which includes coils 25 and 34. The coils in each subgroup are connected in parallel.

In section C3, the coils numbered 8, 9, 26, and 27 are connected in series.

When the three-phase power supply is connected to terminals A, B, and C (while terminals D, E, and F remain open and the contacts of the contactor are disconnected), an eight-pole rotating magnetic field is generated in the air gap. The circuit includes 24 coils; in each phase, the EMF vectors have equal amplitudes and are phase-shifted by 120°, which ensures that the winding for $2p_2 = 8$ poles is completely symmetrical with respect to the power supply.

When the three-phase power supply is connected to terminals D, E, and F (while terminals A, B, and C are open and the contactor contacts are closed), a six-pole rotating magnetic field is formed in the air gap. In this configuration, 36 coils are used; in each phase, the EMF vectors have equal amplitudes and are phase-shifted by 120°, which provides complete symmetry of the winding for $2p_1 = 4$ poles relative to the power supply [11].

To determine the amplitude values of the higher harmonics of the resulting PCW scheme, the following expressions were derived based on the MMF waveform [17], [18].

for $2p_1=8$ poles:

$$F_{vm} = \frac{2}{\pi\nu}(\frac{1}{2}\sin\nu\,10° + \frac{3}{2}\sin\nu\,30° + \sin\nu\,50° + \frac{1}{2}\sin\nu\,70° - \frac{1}{2}\sin\nu\,110° - \sin\nu\,130° - \frac{3}{2}\sin\nu\,150° - \frac{1}{2}\sin\nu\,170°) \quad (1)$$

for $2p_3 = 6$ poles:

$$F_{\nu m} = \frac{4}{\pi\nu}\left(\sin\nu\, 30° + \frac{3}{2}\sin\nu\, 45° + \sin\nu\, 75°\right), \quad (2)$$

for $2p_2 = 4$ poles:

$$F_{\nu m} = \frac{4}{\pi\nu}\left(\frac{1}{2}\sin\nu\, 27° + \frac{3}{2}\sin\nu\, 45° + \frac{3}{2}\sin\nu\, 63° + \frac{1}{2}\sin\nu\, 81°\right). \quad (3)$$

The values of the winding factors and the amplitude of each harmonic, taking these factors into account, are presented in Table 5.

The differential leakage coefficients were determined using the Görges diagram (Fig. 5) [10], [18].

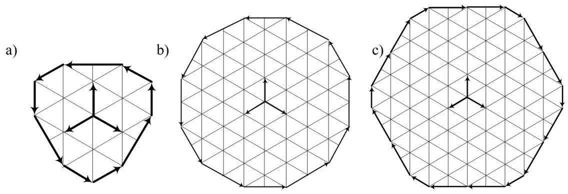

Figure 5: Görges diagram of windings for a three-speed motor: a) for 2p=8; b) for 2p=6; c) for 2p=4.

As can be seen from the MMF waveform, with a coil pitch of y=5, the amplitude value of the fundamental harmonic on the side of p=4 poles is ν_1=97.7% of the total harmonic, while the higher-order harmonic components are minimal (even harmonics are absent). The shape of the Görges diagram is close to a circle, and the value of the differential leakage coefficient is σ_0=5.9% [10, 19]. On the side of p=2 poles, the amplitude value of the fundamental harmonic is ν_1=97.87% of the total harmonic, the higher-order harmonic components are minimal (even harmonics are absent), the Görges diagram is very close to a circle, and the value of the differential leakage coefficient is σ_0 = 1.5% [10], [19], [20].

The analysis shows (Fig. 6) that, for the pole-changing winding based on the 'Y/YY scheme with additional branches,' when the number of pole pairs is *p*=4 and the winding pitch is *y*=5, the amplitude of the fundamental harmonic is relatively high, accounting for 97.7% of the total harmonic content, while higher-order harmonic components are minimal and even harmonics are absent.

Table 5: Harmonic composition of the PCW with a pole ratio of 8/4 at different coil pitches.

ν	$F_{\nu M}/F_{\sum}$,%, taking into account k_w						$F_{\nu M}/F_{\sum}$,%					
	p=8			*p*=4			*p*=8			*p*=4		
	y=4	y=5	y=6	y=4	y=5	y=6	y=4	y=5	y=6	y=4	y=5	y=6
1	97.7	97.7	91.12	91.8	97.87	92.4	100.0	100.0	100.0	100.0	100.0	100.0
3	0.00	0.00	0.00	0.00	0.00	0.00	0.000	0.000	0.000	0.000	0.000	0.000
5	0.28	0.28	0.37	0.27	1.51	0.65	0.291	0.291	0.683	0.291	1.546	1.028
7	1.12	1.12	7.20	1.69	0.02	0.54	1.145	1.145	9.494	1.837	0.017	0.584
9	0.00	0.00	0.00	0.00	0.00	0.00	0.000	0.000	0.000	0.000	0.000	0.000
11	0.71	0.71	5.81	0.67	0.02	0.29	0.729	0.729	6.041	0.729	0.016	0.310
13	0.11	0.11	0.21	0.10	0.58	0.37	0.112	0.112	0.263	0.112	0.595	0.395
15	0.00	0.00	0.00	0.00	0.00	0.00	0.000	0.000	0.000	0.000	0.000	0.000

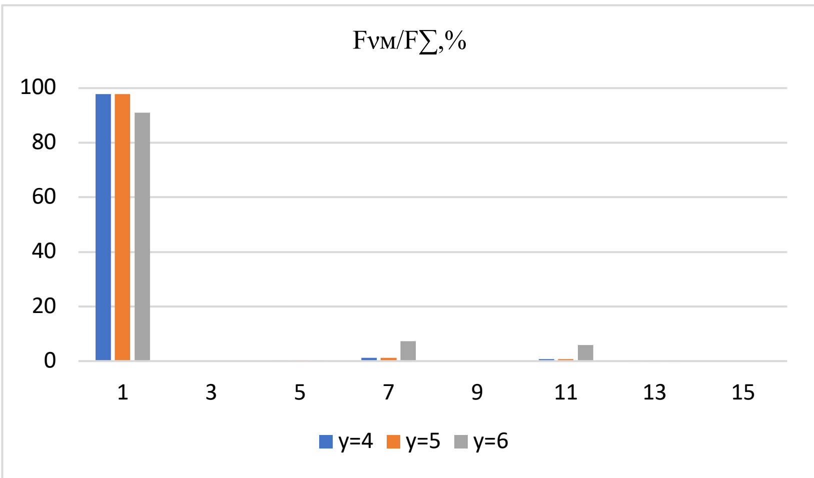

Figure 6: Harmonic spectrum of the magnetomotive force for *p*=4.

3 RESEARCH RESULTS

In a narrow sense, the performance characteristic of an asynchronous motor is understood as the dependence of the rotational speed or slip on the given power. In a broader sense, it includes a number of other parameters important for operation, such as the input power, current, efficiency, and power factor, measured at constant supply voltage and frequency.

The operational characteristics of the electric motor were obtained directly under load conditions for pole numbers p_1=2, p_2=3, and p_3=4 (Tables 6-8).

Table 6: Data on the operating characteristics for the p_1=2 pole configuration.

№	P_2	n	I_1	cosφ	η	M
	kW	rpm	A		%	Nm
1	0.15	1475	1.2	0.27	64	0.9
2	0.2	1472	1.25	0.34	70	1.1
3	0.3	1470	1.32	0.41	77.5	2
4	0.5	1467	1.45	0.59	83	3.1
5	0.75	1460	1.8	0.75	85.5	4.8
6	1	1456	2.1	0.81	85.4	6.5
7	1.25	1452	2.6	0.87	84.2	8.1
8	1.5	1450	3.1	0.9	83.1	9.9
9	1.75	1448	3.55	0.91	80.2	11.5
10	2	1447	4.2	0.915	78	13.2

The results of the experimental studies are presented in Figures 7-8, showing the performance characteristics of the newly developed three-speed motor.

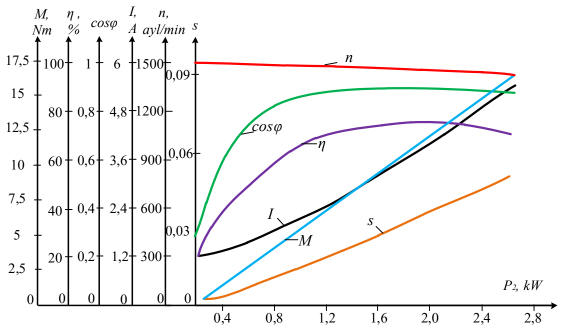

Figure 7: The operating characteristics of the new three-speed motor for the p_1=2 pole configuration.

The results of the experimental studies showed that for the new 4A100S8/6/4 type electric motor, when operating in the p_1=2 pole configuration, the effective output power reaches P_2=1.75 kW, with an efficiency η=80.2%, power factor cosφ=0.91, stator current I_1=3.55 A, and rotor speed n=1448 rpm.

For the p_2=3 pole configuration, the effective output power of the new motor reaches P_2=0.9 kW, with an efficiency η=68%, power factor cosφ=0.64, stator current I_1=3.15 A, and rotor speed n=976 rpm.

Table 7: Data on the operating characteristics for the p_2=3 pole configuration.

№	P_2	n	I_1	cosφ	η	M
	kW	rpm	A		%	Nm
1	0.1	996	2.6	0.24	22	1
2	0.2	993	2.65	0.29	36	2
3	0.3	990	2.69	0.35	46	2.9
4	0.4	986	2.72	0.41	53.8	3.95
5	0.5	984	2.77	0.46	58.2	4.8
6	0.6	982	2.85	0.51	62	5.9
7	0.7	980	2.92	0.56	64.1	6.8
8	0.8	978	3	0.6	66.2	7.9
9	0.9	976	3.15	0.64	68	9
10	1.2	974	3.5	0.74	70	12

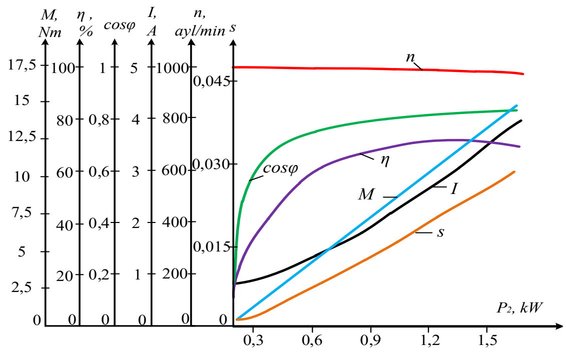

Figure 8: The operating characteristics of the new three-speed motor for the p_2=3 pole configuration.

Table 8: Data on the operating characteristics for the p_3=4 pole configuration.

№	P_2	n	I_1	cosφ	η	M
	kW	rpm	A		%	Nm
1	0.1	745	1.4	0.27	40	1.2
2	0.2	742	1.43	0.38	56	2.5
3	0.3	740	1.5	0.48	64	4
4	0.4	736	1.6	0.56	68	5.2
5	0.5	732	1.73	0.63	68.5	6.5
6	0.6	730	1.9	0.69	69.1	7.7
7	0.7	726	2.1	0.73	68	9.4
8	0.75	722	2.25	0.74	67.8	9.8
9	0.8	720	2.4	0.76	66	10.8

For the p_3=4 pole configuration, the effective output power of the new motor reaches P_2=0.7 kW, with an efficiency η=68%, power factor cosφ=0.73, stator current I_1=2.1 A, and rotor speed n = 726 rpm.

4 CONCLUSIONS

Analysis of the poultry farm microclimate system showed that ventilation equipment consumes up to 54% of the total annual electricity. Therefore, ventilation drives represent the main reserve for improving energy efficiency and reducing operating costs while maintaining required air conditions. Experimental studies confirmed that the use of three-speed motors significantly reduces power consumption. Energy savings reach 74% at 0.5 m/s, 68% at 1.1 m/s, and 52% at 1.5 m/s air velocity. This proves the effectiveness of multi-speed drives for agricultural ventilation systems.

A new 8/4 pole-changing winding was developed based on the improved Y/YY configuration with additional branches using the method of Discrete Specified Phase Functions. The design increases magnetic induction by 19.1% compared to existing solutions and ensures stable operation over a wide airflow range (Patent No. IAP 7673).

REFERENCES

[1] I. M. Dovlatov, A. A. Smirnov, D. Yu. Pavkin, and V. P. Zaikin, "Technology and means for improving the microclimate of livestock premises," Bull. Nizhny Novgorod State Eng. Econ. Inst., no. 4, vol. 107, pp. 34-43, 2020.

[2] Kh. G. Karimov and Yu. A. Tupoguz, "Method of constructing electrically combined windings of alternating current," Elektrichestvo, no. 9, pp. 29-38, 1987.

[3] S. S. Orlova, T. A. Pankova, and O. V. Mikheeva, Design of Ventilation Systems for Livestock and Poultry Complexes. Saratov, Russia: Saratov State Agrarian Univ., 2018.

[4] A. V. Karpenko and I. Yu. Petrova, "Models of indoor microclimate control," Fundamental Research, no. 7, pt. 2, pp. 224-229, 2016, [Online]. Available: https://fundamental-research.ru/ru/article/view?id=40488.

[5] F. Tuychiev and A. Haqberdiev, "Development of two-speed asynchronous electric motors for the undercarriage of mine self-propelled cars," E3S Web Conf., vol. 384, Art. no. 01044, pp. 1-5, 2023, [Online]. Available: https://doi.org/10.1051/e3sconf/202338401044.

[6] G. Kovacs, "A 3Y/3Y pole-changing winding of high-power asynchronous motors," World Acad. Sci., Eng. Technol., Int. J. Electr. Comput. Eng., vol. 12, no. 1, pp. 1367-1374, 2018.

[7] M. Q. Bobojonov, F. N. Tuychyev, N. Rashidov, and A. Haqberdiev, "The possibility of using hybrid winding in doubly fed induction generator," in AIP Conf. Proc., 2024, [Online]. Available: https://doi.org/10.1063/5.0219623.

[8] M. van der Giet, K. Hameyer, and S. Risse, "Induction motor with pole-changing winding for variable supply frequency," in Proc. IEEE Int. Electric Machines & Drives Conf. (IEMDC), 2007, pp. 1484-1489, [Online]. Available: https://doi.org/10.1109/IEMDC.2007.383647.

[9] Kh. Shamsutdinov, "Study on improving the asynchronous electric drive of ball mills," in E3S Web Conf., vol. 497, Art. no. 01001, 2024, [Online]. Available: https://doi.org/10.1051/e3sconf/202449701001.

[10] M. Caruso, A. O. Di Tommaso, F. Marignetti, R. Miceli, and G. R. Galluzzo, "A general procedure for the construction of Gorges polygons for multi-phase windings of electrical machines," in Proc. 13th Int. Conf. Ecological Vehicles Renewable Energies (EVER), Apr. 2018, pp. 1-7, [Online]. Available: https://doi.org/10.1109/EVER.2018.8362348.

[11] A. Haqberdiev and J. Toshov, "Analysis of the control system of electric motors of the running gear of self-propelled mine wagons used in complex mining and technological conditions," E3S Web Conf., vol. 216, Art. no. 01135, 2020, [Online]. Available: https://doi.org/10.1051/e3sconf/202021601135.

[12] V. N. Vanurin, Stator Windings of Asynchronous Electrical Machines, 2nd ed., rev. and exp. St. Petersburg, Russia: Lan Publ., 2016.

[13] V. N. Vanurin, N. I. Bogatyriev, and O. V. Vronskii, Stator Winding Schemes, Parameters, and Characteristics of AC Electrical Machines. Krasnodar, Russia: Krasnodar Tech. Univ. Press, 2007.

[14] V. N. Vanurin, Stator Windings of Multi-Speed Electric Motors. St. Petersburg, Russia: Lan Publ., 2022.

[15] M. Q. Bobojonov, F. N. Tuychyev, N. Rashidov, A. Haqberdiev, and S. To'rayev, "Increasing energy efficiency through the use of combined windings in induction machines," in AIP Conf. Proc., vol. 3331, Art. no. 020005, 2025, [Online]. Available: https://doi.org/10.1063/5.0305749.

[16] E. Libbos, E. Krause, A. Banerjee, and P. T. Krein, "Winding layout considerations for variable-pole induction motors in electric vehicles," IEEE Trans. Transport. Electrific., vol. 9, no. 4, pp. 5214-5225, 2023.

[17] K. S. Chettiar, R. Dhanushkodi, and S. Narayanan, "Electro-thermal co-design of a variable-pole toroidal induction motor," Appl. Thermal Eng., early access, 2024.

[18] D. A. Rismukhamedov, Kh. F. Shamsutdinov, Kh. Rozmetov, Sh. Khusanov, and S. D. Rismukhamedov, "Improvement of electromagnetic properties of pole-changing windings," in AIP Conf. Proc., vol. 3331, Art. no. 040058, 2025, [Online]. Available: https://doi.org/10.1063/5.0305959.

[19] E. V. Goremykin, Electrical Equipment of Industry. Part 2: Industrial Electric Drive. Taganrog, Russia: Taganrog State Radio Eng. Univ. Press, 2005.

[20] N. F. Kotelenets, N. A. Akimov, and M. V. Antonov, Testing, Operation, and Maintenance of Electrical Machines. Moscow, Russia: Academy Publ., 2003.